Optik - International Journal for Light and Electron Optics 272 (2023) 170214

Contents lists available at ScienceDirect

Optik

journal homepage: www.elsevier.com/locate/ijleo

Bismuth(III) oxide and boron(III) oxide substitution in bismuth-boro-zinc glasses: A focusing in nuclear radiation shielding properties

Ghada ALMisned [a], Ghaida Bilal [b], Duygu Sen Baykal [c], Fatema T. Ali [d], G. Kilic [e], H.O. Tekin [b,f,*]

[a] Department of Physics, College of Science, Princess Nourah Bint Abdulrahman University, P.O. Box 84428, Riyadh 11671, Saudi Arabia
[b] Department of Medical Diagnostic Imaging, College of Health Sciences, University of Sharjah, 27272 Sharjah, United Arab Emirates
[c] Istanbul Kent University, Vocational School of Health Sciences, Medical Imaging Techniques, Istanbul 34433, Turkey
[d] Center for Advanced Materials Research (CAMR), Research Institute of Sciences and Engineering, University of Sharjah, Sharjah 27272, United Arab Emirates
[e] Eskisehir Osmangazi University, Faculty of Science, Department of Physics, Eskişehir, Turkey
[f] Istinye University, Faculty of Engineering and Natural Sciences, Computer Engineering Department, Istanbul 34396, Turkey

ARTICLE INFO

Keywords:
Bismuth oxide
Glass shield
Nuclear radiation
Radiation protection

ABSTRACT

Doping the glass structure with Bi_2O_3 `is known to increase structural stability, and to drastically alter physical parameters including density and molar volume. The goal of this work was to assess the nuclear radiation attenuation competences of several types of glasses based on the xBi_2O_3-(70-x)B_2O_3-8BaO-16ZnO-5.5SiO_2- 0.5Sb_2O_3 system. In order to determine the requisite gamma shielding parameters, as well as effective conductivity at 300 K and buildup factors, five different glasses with varied Bi_2O_3 concentration (i.e., from 10 mol.% to 30 mol.%) were examined thoroughly. These critical parameters were determined using the Phy-X/PSD program. In addition, factors such as half value layer (HVL), tenth value layer (TVL), and mean free path (mfp) were examined over a wide energy range of 0.015–15 MeV. The findings revealed that the amount of Bi_2O_3 reinforced in each sample is critical in determining the samples' shielding abilities. The linear attenuation coefficients (μ) and mass attenuation coefficient (μ_m) values were reported in the highest level for the sample with the highest Bi_2O_3 content. For glass sample A5, the lowest mean free path, half value layer, and tenth value layer values were also reported. The effective conductivity and effective atomic number had an inverse relationship with photon energy, meaning that as energy increased, the effective conductivity and effective atomic number declined fast, especially in low-energy regions. The greatest values for both parameters were found in glass sample A5. Furthermore, the exposure buildup factor and energy absorption buildup factor values for glass sample A5 were the lowest. A5 glass sample with the chemical composition 30Bi_2O_3-(70−30) B_2O_3-8BaO-16ZnO-5.5SiO_2- 0.5Sb_2O_3 and a density of 5.8391 g/cm^3 was found to have exceptional gamma-ray attenuation qualities, according to our findings. It can be concluded that the prospective attributes of Bi_2O_3-doped glass systems and associated glass compositions would be beneficial for scientific community in terms of providing a clearer view for some advanced applications of these glass types.

* Corresponding author at: Department of Medical Diagnostic Imaging, College of Health Sciences, University of Sharjah, 27272 Sharjah, United Arab Emirates.
E-mail address: tekin765@gmail.com (H.O. Tekin).

https://doi.org/10.1016/j.ijleo.2022.170214
Received 19 September 2022; Accepted 7 November 2022
Available online 8 November 2022

1. Introduction

Industries, medical physics, and nuclear research facilities all benefit greatly from nuclear technology. Besides these fields, advanced applications of nuclear technologies can be found in agriculture and food technologies, such as plant gene mutation and food preservation; medicine and nondestructive testing via radiography; radiation shielding and radiation dosimetry via structural characterization of materials; and so on. On the other hand, widespread reliance on radiation does not mean that the risks associated with it are disregarded. While widespread use of ionizing radiation is not yet a reality, there is a significant increase in the quantity of radiation released by artificial sources to society and the environment. Radiation has a significant ability to permeate the human body, which can cause damage directly or indirectly through distortion and inheritance to future generations. As a result, individuals have made significant attempts to limit ionizing radiation's harmful effects. One of them is to investigate shielding materials, which encourages scientists to develop novel shielding materials. Lead and concrete have been proven to be among the most effective materials in this field after extensive study of their radiation attenuation capabilities by several studies. This is owing to lead and concrete's high densities and, as a result, their high ability to attenuate photons and diminish their intensity. Despite their high photon attenuation ability, these materials have several drawbacks that prevent them from being used in numerous practical applications. These drawbacks stem from lead's high weight, which makes it difficult to wear as an apron since it strains the spine; also, lead and concrete are opaque materials, making it hard to construct face shields or eye protection from them. Most importantly, lead's toxicity has resulted in its categorization as a hazardous substance with unfavorable environmental consequences. Concrete is an affordable, durable material that provides a great resistance against X-rays and gamma-rays. On the other hand, concrete that has been subjected to radiation is more likely to fracture and lose its moisture content. Instead, glass is one of the most promising materials that has been shown to be effective in radiation shielding. To replace concrete and lead, glass is a viable option because to its transparency, high homogeneity, and simplicity of manufacture. As they can accommodate a broad variety of heavy metal components in their matrix, glass materials show great promise as radiation shields. Since a consequence, several types of glass have found employment in nuclear applications in recent years, as they may serve as both a transparent radiation shield and a protective barrier. Both its rigidity and its optical characteristics should be somewhat unaffected by irradiation. Glasses' attenuation capacity may be improved by doping them with heavy metal oxides (HMOs) or dense metal oxides. Previous studies have indicated that density is positively correlated with attenuation effectiveness. Lead glass, which is readily accessible, is often used for shielding against nuclear radiation [1–12]. However, lead's toxicity meant that drinking out of lead glasses was discouraged. Radiation shielding glasses devoid of lead have been the subject of several research efforts [13]. Due to its versatility, bismuth oxide glasses have lately gained a lot of interest. High density, high refractive index, high dielectric constant, and so on are all properties of the produced glasses. In light of this, scientists are curious in the synthesis, physical features, and radiation attenuation qualities of glasses containing bismuth oxide [14–16]. Mohammad and Bektasoglu [17] investigated the role that bismuth borate glasses played in determining the gamma-ray shielding capacities of the glass system, and they found that increasing the quantity of bismuth in the glasses improved their attenuation properties. Bismuth is a realistic option since it is an HMO with shielding properties comparable to lead's, with the extra bonus of being environmentally benign. Bismuth-based glasses, which have a greater mass attenuation coefficient and half-value layer properties, may be preferable to lead-based glasses for gamma ray shielding applications. Glass modifiers are introduced to the system in order to alter the properties of the glass. ZnO is one of several transition metal oxides utilized as a chemical intermediate. To alter the system's shielding characteristics, glass modifiers may lower the melting point and viscosity without changing the system's chemical properties. Glass with the highest concentration of Bi2O3 was found to have the greatest shielding characteristics in an investigation by Sayyed et al. [18] into the properties of a tellurite germanate glass system including Li_2O, ZnO, and Bi2O3. The goal of this research is to find a suitable replacement for lead or lead-based shielding materials in nuclear medicine facilities and develop an innovative, highly effective, and environmentally conscious alternative. In the study by Liu et. al. in which 5 glass structures having Bi_2O3-B_2O_3-BaO-ZnO [19] composition containing different ratios of Bi_2O_3, glass structures and changes in the density, molar volume and thermal properties were focused on. Increasing Bi2O3 ratio was both determined to improve the chemical stability of the glass and also increase the density significantly. These favorable changes were considered to have positive impact on radiation shielding properties, thus the effectiveness of shielding against diagnostic radiation in nuclear medicine was studied by analyzing these 5 different glass samples with Bi_2O_3 contents between 10% and 30%. In this research, we characterized the gamma-ray shielding characteristics of this xBi_2O_3-(70-x) B_2O_3-8BaO-16ZnO-5.5SiO_2-0.5Sb_2O_3 glass system. Each sample's efficacy and superiority will be scrutinized and debated as the additive concentration increases.

Table 1
Sample codes, composition, elemental weight fractions and densities of the glass samples.

Sample code	B	O	Si	Zn	Sb	Ba	Bi	g/cm^3
A1	0.186343	0.493873	0.025709	0.128548	0.004177	0.071652	0.089699	4.111
A2	0.170814	0.464552	0.025709	0.128548	0.004177	0.071652	0.134548	4.6973
A3	0.155285	0.435231	0.025709	0.128548	0.004177	0.071652	0.179398	5.0905
A4	0.139757	0.40591	0.025709	0.128548	0.004177	0.071652	0.224247	5.5821
A5	0.124228	0.376589	0.025709	0.128548	0.004177	0.071652	0.269097	5.8391

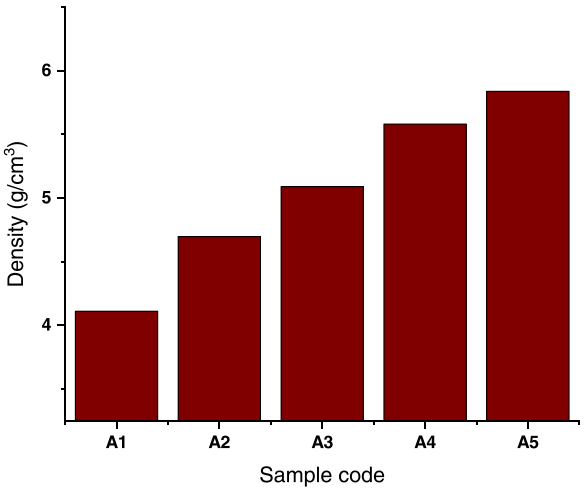

Fig. 1. Variation of glass densities from A1 to A5.

2. Materials and methods

The gamma ray shielding properties of five different glasses with the chemical composition xBi_2O_3-(70-x)B_2O_3-8BaO-16ZnO-5.5SiO_2-0.5Sb_2O_3 (Where x = 10–30 mol.%) were extensively investigated. Glass samples A1, A2, A3, A4, and A5 were made using the conventional melt-quenching technique, as described in the cited research [19]. Densities of Glass Samples A1, A2, A3, A4, and A5 were reported to be 4.111 g/cm^3, 4.6973 g/cm^3, 5.0905 g/cm^3, 5.5821 g/cm^3, and 5.8391 g/cm^3 in the cited research [19]. (See Table 1). Here, one can see the technical details and the computed parameters for nuclear radiation shielding. Radiation attenuation parameters of the samples were calculated using Phy-x PSD software [20].

2.1. Investigated nuclear radiation shielding properties of glass samples

The mass attenuation coefficient may be simplified by knowing the Lambert-Beer law, which is expressed in Eq. 1.

$$I = I_o e^{-\mu t} \tag{1}$$

Primary radiation intensity (I_0), attenuated radiation intensity (I), attenuator thickness (t), and the linear radiation attenuation coefficient (μ) are all represented by the equation. [21]. Using the measured μ values, we calculated the glass samples' density-independent radiation attenuation property by computing their mass attenuation coefficients (μ_m) [22].

$$\mu_m = \frac{\mu}{\rho} \tag{2}$$

After passing through an attenuator material, a photon typically travels a distance equal to its mean free path (mfp), which can be calculated with the help of Eq. 3.

$$MFP = \frac{1}{\mu} \tag{3}$$

Based on Eq. 5, the half value layer (HVL) is the thickness of the attenuator required to lower the radiation intensity by half.

$$HVL = \frac{ln \quad (2)}{\mu} \tag{4}$$

The thickness of the attenuator needed to lower the radiation intensity by a tenth is referred to as the tenth value layer (TVL) [23,24]. In order to calculate it, we use Eq. 5:

$$TVL = \frac{ln \quad (10)}{\mu} \tag{5}$$

The technical and theoretical information about the critical gamma-ray absorption parameters calculated in this study can be obtained from previous studies in the literature and, elsewhere [25–30] (Fig. 1).

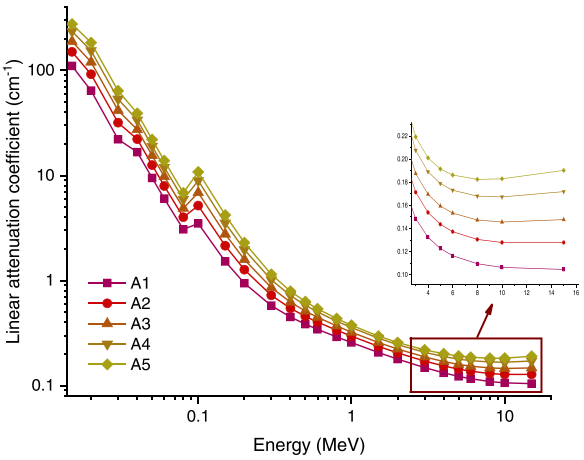

Fig. 2. Variations of linear attenuation coefficients (cm^{-1}) as a function of photon energy (MeV) for A1-A5 glasses.

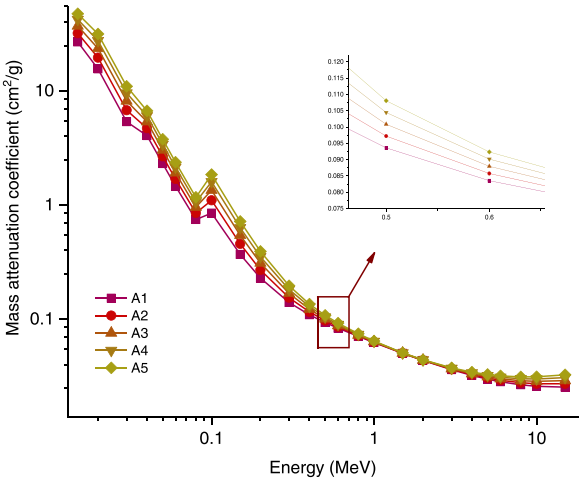

Fig. 3. Variations of mass attenuation coefficients (cm^2/g) as a function of photon energy (MeV) for A1-A5 glasses.

3. Results and discussion

In this work, the gamma-ray attenuation properties of five distinct glass samples were thoroughly studied using various types of critical calculations. The samples were previously prepared from a system consisting of xBi_2O_3-(70-x) B_2O_3-8BaO-16ZnO-5.5SiO_2-0.5Sb_2O_3 (Where x = 10–30 mol. %). The variation in the linear attenuation coefficient (μ) of the analyzed glass samples is shown as a function of photon energy in Fig. 2. Photons can get their energy in one of two methods, both of which include certain types of interactions between the incident photons and the electrons on the orbit of the atoms. Through one situation, the photon is completely absorbed, but in the other, just a portion of the photons are absorbed, allowing the rest to be scattered [31]. It would appear that photons with lower energies (0.1 MeV) have been greatly affected from photoelectric effect. The probability of this interaction occurring substantially rises with each successively higher atomic number. When photons have a medium to high energy (i.e., more than 0.1 MeV), the Compton effect may be seen most effectively. When photons have an energy that is more than 1.02 MeV, a phenomenon known as pair production may take place. It is acceptable to suppose that the linear attenuation coefficient is energy-dependent and varies with the energy of the photon given the sorts of interactions that have been described. Fig. 2 depicts the variation of the linear attenuation coefficients as a function of incident photon energy (MeV). It is seen that a sharp drop between the 0.015 MeV and 0.08 MeV, which is the zone where the photoelectric impact is most frequent. The first zone in the graph exhibited a gradual decline, much as the second zone, which referred to the predominance of Compton scattering and exhibited a smooth drop. Based on the findings, it seems that the values for the A5 glass sample were the highest. The presence of Bi_2O_3 in the sample provides sufficient evidence to support this assumption. When compared to the other samples, A5 stands out as having the greatest density (i.e., 5.8391 g/cm3) as well as the highest percentage of Bi_2O_3 amount in its structure (see Table 1). The increase in the amount of Bi_2O_3 that was present in the glass samples was responsible for the precipitous increase in density. The sample with 10 mol.% Bi_2O_3 (also known as A1) has the lowest density (4.111 g/cm^3) among the investigated glass samples, while the sample with 30 mol.% Bi_2O_3 (also known

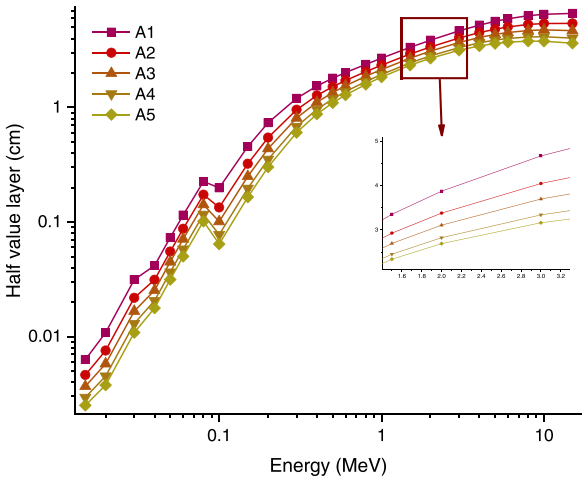

Fig. 4. Variations of half value layer (cm) as a function of photon energy (MeV).

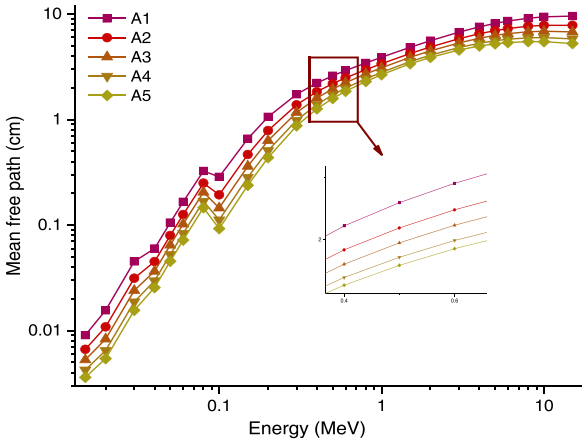

Fig. 5. Variations of mean free path (cm) values as a function of photon energy (MeV) for A1-A5 glasses.

as A5) has the greatest density (5.8391 g/cm^3) This situation is driven about by the fact that Bi has a greater atomic number than Z, which is equal to 80. In Fig. 3, we illustrated that how the mass attenuation coefficients (μ_m) varies as a function of the energy of the photon. One way to express the rate of attenuation is to consider it in terms of the mass of the substance that photons collide with. The mass of an attenuator's total area, rather than its total mass, is the factor that determines the rate of attenuation it produces [32]. The mass attenuation coefficient is a criterion for assessing the shielding qualities of a material that is independent of the substance's density. In this research, the values of the samples' μ_m were estimated using photon energy ranges that ranged from 0.015 MeV all the way up to 15 MeV. Fig. 3 depicts the distribution of μ_m as a function of the incoming photon energy for all of the glass samples that were investigated. There is a variation pattern that can be compared to the one observed in μ values. The prevalence of the aforementioned interactions was also given in terms of their μ values. The density of the glass samples has been shown to exhibit gradual fluctuations, which may be the cause of this similarity. A similar trend is expected because μ_m values can be calculated by dividing density by μ. The variation in μm values has been shown to be affected by the incoming photon energy as well as the chemical compositions of the glass samples. The difference in energy levels is clearly discernible across three distinct zones. In the low energy range, where the photo-electric effect is the predominate mechanism in the interaction, the μm values drop down dramatically as the gamma energies increase. The rate of decrease slowed down as the energy increased. In the second area, the predominance of Compton scattering showed an equivalent declining trend. On the other hand, it was found that the values of μ_m decreased as the gamma-ray energy increased. Sample A5 has the highest μ_m values across the range for the various photon energies. For example, the values of μ_m were reported to be 0.850, 1.101, 1.352, 1.602, and 1.853 cm^2/g for glass samples A1, A2, A3, A4, and A5, respectively, when exposed at 0.8 MeV gamma-ray energy. The increase in the mass attenuation coefficient that is brought on by a greater concentration of Bi_2O_3 might be connected to a larger mole fraction of a component with a higher atomic number (Bi) in contrast to the mole fractions of other elements. Research on radiation shielding uses an essential term namely HVL, which is also known by the notation $T_{1/2}$. This term is significant since it enables the calculation of the minimum required thickness of the shielding material that should be used to reduce the primary

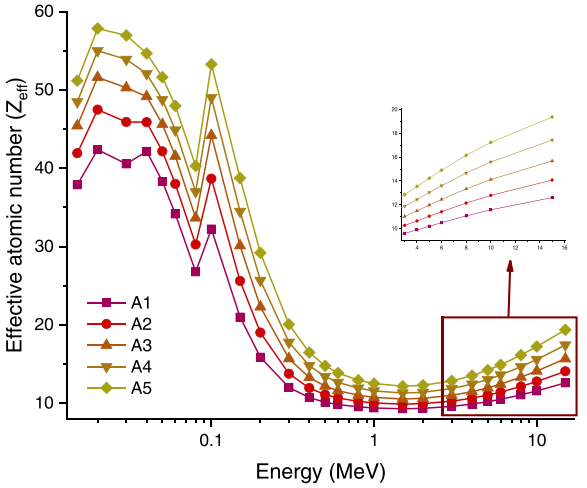

Fig. 6. Variations of effective atomic number (Z_{eff}).

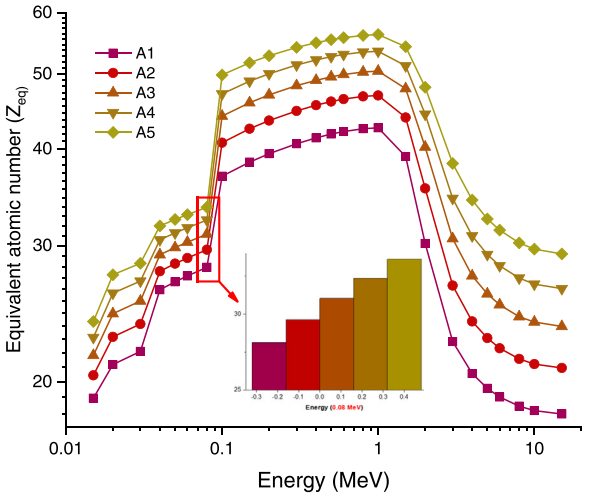

Fig. 7. Variations of equivalent atomic number (Zeq) values.

gamma-ray intensity to its half. This is because radiation-based investigations need selecting the most proper shield in advance depending on the type and energy of the radiation that is being utilized. As a consequence of this situation, the quantity of HVL required for every possible form of shielding material has to be determined. Fig. 4 shows the relationship between the incoming photon energy and the HVL (cm) values of the different glasses that were investigated. The linear attenuation coefficients and the HVL values have an inverse connection with one another. Eventually, it is reasonable to suppose that the sample with the greatest values of the linear attenuation coefficient would have the lowest values of the HVL. According to the results of this study, the A5 sample had the highest density and linear attenuation coefficients, although having the lowest HVL values. For instance, the HVL values reported for glass samples A1, A2, A3, A4, and A5 at 0.1 MeV were correspondingly 0.198, 0.134, 0.101, 0.077, and 0.064 cm. The MFP values, on the other hand, for the various glass samples that were analyzed are shown in Fig. 5. The MFP, along with the HVL, should be as low as possible. As the mean free path (MFP) becomes smaller, the distance between two consecutive contacts gets shorter, which suggests that the attenuation ability of materials of equivalent thickness becomes more relevant. Therefore, the performance of each and every gamma-ray shielding media may be directly represented by the MFP value [33]. Fig. 6 illustrates the variation that occurs in the values of the effective atomic number (Z_{eff}) of the glass samples that were tested as a function of the input photon energy (MeV). According to Fig. 6, the sample A5 has the greatest Z_{eff} values, while the sample A1 has the lowest Z_{eff} values. These results can be seen by comparing the two samples. This is due to the fact that Z_{eff} increases as the amount of Bi_2O_3 present is increased ($Z = 83$). According to our data, the point at which the Z_{eff} value was at its highest for the A5 sample was 0.02 MeV, and it was 57.84. In addition, the peak seen at around 0.1 MeV may be due to Bi's k-absorption edge being responsible for it. In order to compute the exposure buildup factor (EBF) and the energy absorption buildup factor (EABF), the geometric progression (G-P) fitting method was used. This resulted in the establishment of equivalent atomic numbers (Z_{eq}) for the five different types of glasses. The variant of Z_{eq} is seen in Fig. 7. According to

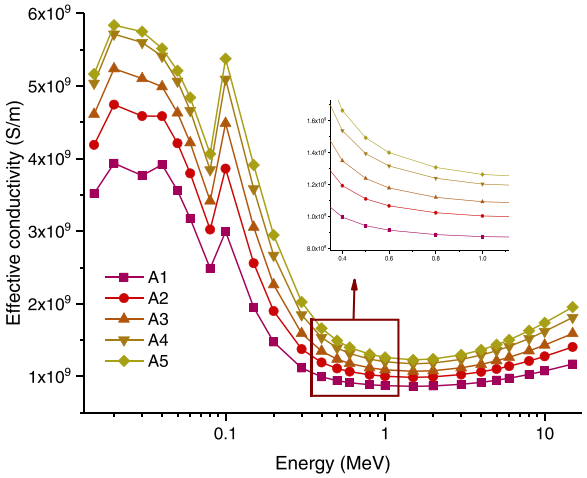

Fig. 8. Variations of effective conductivity at 300 Kelvin (S/m).

the given graph, there was a discernible rise in the amount of activity in the low-energy zone. Thereafter, there was an abrupt decline up to the photon energy of 1 MeV, which was then followed by a slow decrease. At 1 MeV, the greatest Z_{eq} values that were recorded were 42.59, 46.88, 50.42, 53.48, and 56.21 for glass samples with the designations A1, A2, A3, A4, and A5, respectively. Despite this, the A5 sample had the greatest Z_{eq} values across the board for the various photon energies. Fig. 8 illustrates how the effective conductivity (C_{eff}) varies across all glass samples when measured at 300 K (s/m). An attenuating shielding material's effective conductivity C_{eff} (s/m) is proportional to the effective electron number per gram when measured at a temperature of 300 K, which corresponds to room temperature. As can be observed in Fig. 8, the C_{eff} values experience a rapid decrease with increasing photon energy, particularly in the zone, where photoelectric interactions are dominant [34]. In addition, the sample with the largest amount of Bi_2O_3, sample A5, also has the highest C_{eff} values across the board for all photon energies. Meanwhile, the term of buildup factor is a correction factor for dispersed radiation that compensates for secondary particles in the medium. It is sometimes referred to as the buildup coefficient. It is necessary to take into consideration the factors of accumulation in order to properly account for the accumulation of secondary ionizing radiation. As a consequence of this, the buildup factor is a multiplier that takes into consideration both the contribution of scattered photons and the reaction to photons that have not been scattered. There are two sub-definitions of the word "buildup factor." These sub-definitions are the exposure buildup factor (EBF) and the energy absorption buildup factor (EABF). The G-P fitting method was used to determine the EBF and EABF values of five different glass samples, and the results ranged between 0.5 and 40 mfp. The variation of EBF and EABF values shown in Fig. 9 as a function of energy, measured in MeV, for a range of different mfp values. When the incoming photon energies are lower, the depth-dependent absorption rises until it reaches a maximum in the intermediate energy range, after which it begins to decline. This continues until the incident photon energies are high enough to cause a reduction. The vast majority of gamma-ray absorption takes place at energies lower than that at which the photoelectric effect is predominate and energies higher than that at which pair formation interactions are predominate. In certain energy zones, the accumulation of photons is restricted. However, at intermediate energies, the process that is most often seen is called Compton scattering. This mechanism includes photon absorption but does not result in an absolute loss of photons. As a direct consequence of this, EBF levels in the Compton region have reached an all-time high. In the course of this investigation, it was discovered that sample A5 had the lowest EBF values. It is important to take note that the EBF values will drop to a lower level as the sample's amount of Bi_2O_3 increases. For example, the EBF values for glass samples A, A2, A3, A4, and A5 were reported to be 60.788, 48.511, 40.267, 34.110, and 29.376 at 1 MeV and 40 MFP, respectively. These values were found to be the highest at 1 MeV. The variance in EABF is also seen in Fig. 9 for A1-A5 glasses. The fluctuation pattern that is seen by EABF is somewhat comparable to that of EBF. In a similar manner, the values are lowest for sample A5, which has the greatest concentration of Bi_2O_3.

4. Conclusion

It is known that doping the glass structure with Bi_2O_3 renders the glass structure more stable, in addition it is known to significantly change physical properties such as density and molar volume. Considering that increase in Bi_2O_3 in the glass structure having Bi_2O_3-B_2O_3-BaO-ZnO composition would increase glass density significantly and would also change and improve radiation shielding properties of the glass distinctly, we have focused on the radiation shielding properties of 5 samples from the abovementioned glass series. Across a broad spectrum of input photon energy, we set out to compare the nuclear attenuation shielding capabilities of five glasses belonging to the xBi_2O_3-(70-x) B_2O_3-8BaO-16ZnO-5.5SiO_2-0.5Sb_2O_3 system (0.015–15 MeV).

- The density of the samples increases linearly from 4.111 g/cm^3 to 5.8391 g/cm^3 when the amount of Bi_2O_3 in the samples rises from 10% to 30%.

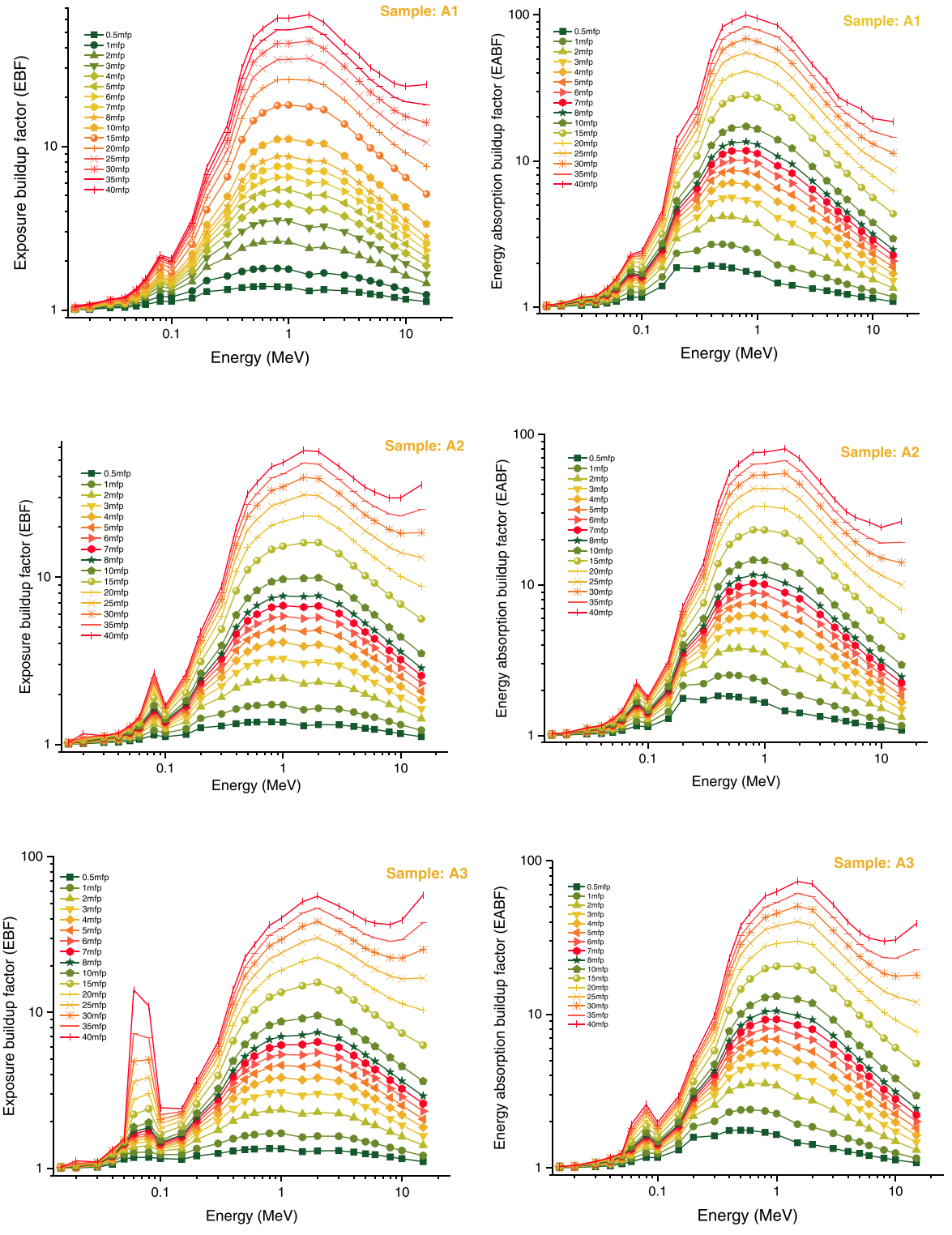

Fig. 9. Variation of exposure buildup factors (EBF) and energy absorption buildup factor (EABF) of investigated glasses at different mean free path values (from 0.5 mfp to 40 mfp).

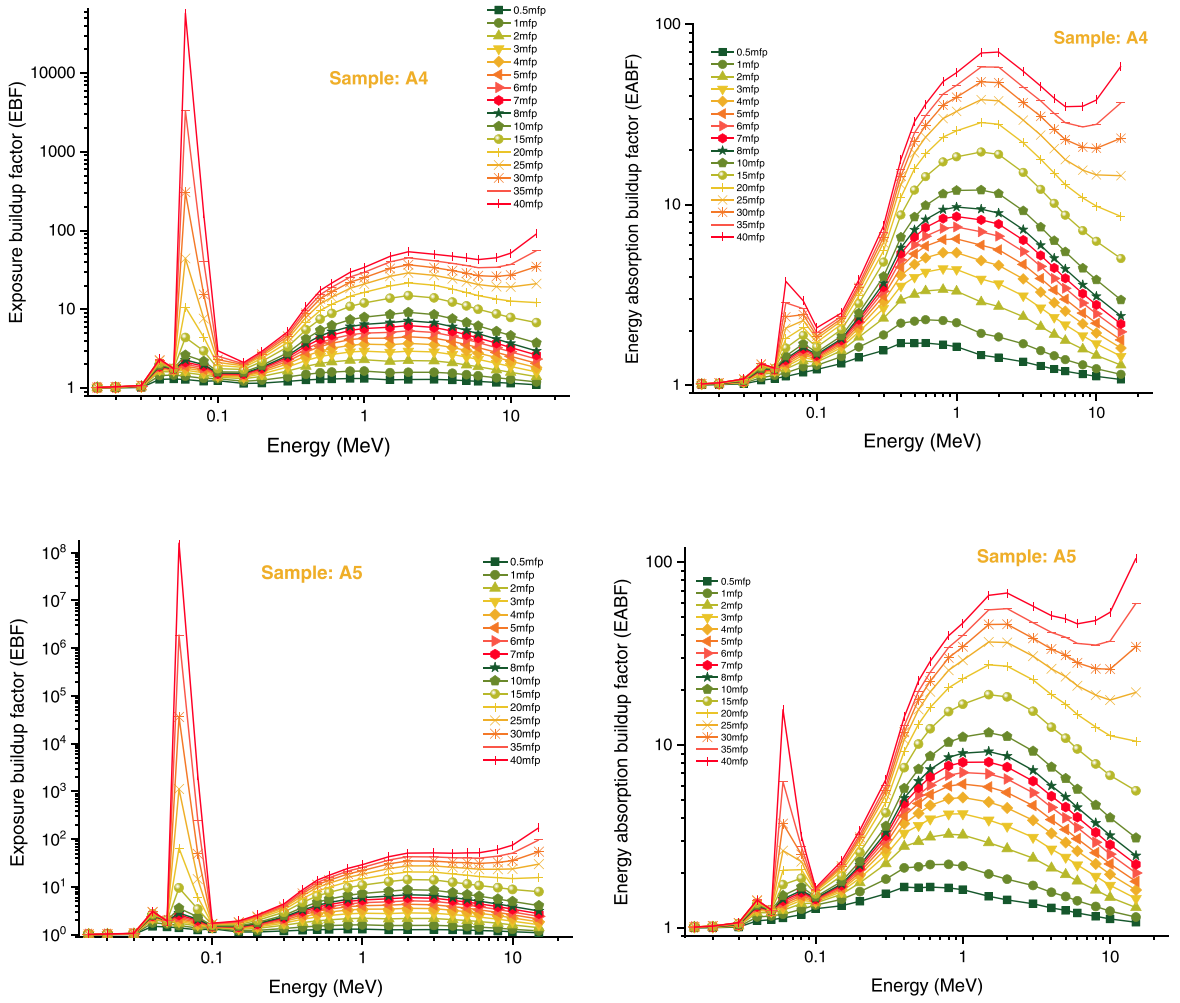

Fig. 9. (*continued*).

- The greatest attenuation of gamma rays was seen in the sample with the highest Bi_2O_3 concentration, demonstrating that Bi_2O_3 reinforcement has a great potential in terms of improving the anti-nuclear radiation characteristics.

We may further describe the results of this investigation as follows: the μ_m values at 0.8 MeV were 0.850, 1.101, 1.352, 1.602, and 1.853 cm2/g for glass samples A1, A2, A3, A4, and A5, with the greatest values found in glass sample A5. Based on our results, sample A5 had the minimum $T_{1/2}$ values throughout the whole spectrum of photon energies investigated. Further, both the Z_{eff} and C_{eff} values for sample A5 were the highest of all the samples. Sample A1 (10 mol. % Bi_2O_3) was found to have the highest EBF and EABF values, whereas sample A3 (30 mol. %) was claimed to have the lowest (i.e., A5). We found that the A5 glass sample is better at absorbing the incident nuclear radiation type, demonstrating that the addition of Bi_2O_3 to the glasses significantly improves their already good shielding qualities. Finally, we would like to provide some suggestions for follow-up research that may be conducted as part of the scientific community's continued work on the present promising glass system. In this study, we provided in-depth findings after considering a variety of factors. While the suggested glassy system shows promise, it will need continued optimization and improvement due to the considerable material features associated with glass materials. A general view of the Bi_2O_3 incorporated glasses samples was provided based on the information supplied. The proposed glass system, however, requires ongoing work in terms of overall optimization and improvement because of the significant material attributes associated with glass components.

Declaration of Competing Interest

None.

Data availability

Data will be made available on request.

Acknowledgement

The authors extend their appreciation to the Deputyship for Research & Innovation, Ministry of Education in Saudi Arabia for funding this research work through the project number RI-44-0001

References

[1] A.S. Abouhaswa, U. Perisanoglu, H.O. Tekin, E. Kavaz, A.M.A. Henaish, Nuclear shielding properties of B2O3–Pb3O4–ZnO glasses: multiple impacts of Er2O3 additive, Ceram. Int. 46 (17) (2020) 27849–27859.
[2] G. ALMisned, H. Zakaly, S. Issa, A. Ene, G. Kilic, O. Bawazeer, et al., Gamma-ray protection properties of bismuth-silicate glasses against some diagnostic nuclear medicine radioisotopes: a comprehensive study, Materials 14 (21) (2021) 6668, https://doi.org/10.3390/ma14216668.
[3] A. Almuqrin, M. Sayyed, N. Prabhu, S. Kamath, Influence of Bi2O3 on mechanical properties and radiation-shielding performance of lithium zinc bismuth silicate glass system using Phys-X Software, Materials 15 (4) (2022) 1327, https://doi.org/10.3390/ma15041327.
[4] A.I. Elazaka, H.M.H. Zakaly, S.A.M. Issa, M. Rashad, H.O. Tekin, H.A. Saudi, V.H. Gillette, T.T. Erguzel, A.G. Mostafa, New approach to removal of hazardous Bypass Cement Dust (BCD) from the environment: 20$Na^{2}O$–^{20}BaCl2-(60-x)B2O3-(x)BCD glass system and Optical, mechanical, structural and nuclear radiation shielding competences, J. Hazard. Mater. (2021) 403–123738, https://doi.org/10.1016/j. jhazmat.2020.123738.
[5] A. El-Denglawey, H. Zakaly, K. Alshammari, S. Issa, H. Tekin, W. AbuShanab, Y. Saddeek, Prediction of mechanical and radiation parameters of glasses with high Bi2O3 concentration, Results Phys. 21 (2021), 103839, https://doi.org/10.1016/j.rinp.2021.103839.
[6] S. Gowda, S. Krishnaveni, T. Yashoda, T.K. Umesh, R. Gowda, Photon mass attenuation coefficients, effective atomic numbers and electron densities of some thermoluminescent dosimetric compounds, Pramana 63 (2004) 529–541, https://doi.org/10.1007/BF02704481.
[7] M. Kurudirek, N. Chutithanapanon, R. Laopaiboon, C. Yenchai, C. Bootjomchai, Effect of Bi2O3 on gamma ray shielding and structural properties of borosilicate glasses recycled from high pressure sodium lamp glass, J. Alloy. Compd. 745 (2018) 355–364, https://doi.org/10.1016/j.jallcom.2018.02.158.
[8] E. Lacomme, M. Sayyed, H. Sidek, K. Matori, M. Zaid, Effect of bismuth and lithium substitution on radiation shielding properties of zinc borate glass system using Phy-X/PSD simulation, Results Phys. 20 (2021), 103768, https://doi.org/10.1016/j.rinp.2020.103768.
[9] E. Şakar, Ö. Özpolat, B. Alım, M. Sayyed, M. Kurudirek, Phy-X / PSD: development of a user friendly online software for calculation of parameters relevant to radiation shielding and dosimetry, Radiat. Phys. Chem. 166 (2020), 108496, https://doi.org/10.1016/j.radphyschem.2019.108496.
[10] H.O. Tekin, M.I. Sayyed, E.E. Altunsoy, T. Manici, Shielding properties and effects of WO3 and PbO on mass attenuation coefficients by using MCNPX code, Dig. J. Nanomater. Biostruct. 12 (2017) 861–867.
[11] I.I. Bashter, A.S. Makarious, Abdo ES. Investigation of hemati-te–serpentine and ilmenite-limonite concretes for reactorradiation shielding, Ann. Nucl. Energy 23 (1) (1996) 65–71.
[12] A.M. Mostafa, S.A. Issa, H.M. Zakaly, M.H. Zaid, H.O. Tekin, K.A. Matori, et al., The influence of heavy elements on theionizing radiation shielding efficiency and elastic properties of some tellurite glasses: theoretical investigation, Results Phys. 19 (2020), 103496.
[13] G. Singh, M.K. Gupta, A.S. Dhaliwal, K.S. Kahlon, Measurement of attenuation coefficient, effective atomic number and electron density of oxides of lanthanides by using simplified ATM-method. J. Alloy. Compd. 2015;619:356–360. S.A. Issa, Effective atomic number and mass attenuation coefficient of PbO–BaO–B2O3 glass system. Radiat. Phys. Chem. 2016;120:33–37.
[14] K. Mann, γ-ray shielding behaviors of some nuclear engineering materials, Nucl. Eng. Technol. 49 (4) (2017) 792–800, https://doi.org/10.1016/j.net.2016.12.016.
[15] A.M. Ali, S.A.M. Issa, M.R. Ahmed, Y.B. Saddeek, M.H. Mohd Zaid, M. Sayed, H.H. Somaily, H. Ozan Tekin, H.A. Aziz Sidek, K.A. Matori, H.M.H. Zakaly, Promising applicable heterometallic Al2O3/PbO2 nanoparticles in shielding properties, J. Mater. Res. Technol. 9 (6) (2020) 13956–13962, https://doi.org/10.1016/j.jmrt.2020.09.125.
[16] G. Kilic, F.I. El Agawany, B.O. Ilik, K.A. Mahmoud, E. Ilik, Y.S. Rammah, Ta2O5 reinforced Bi2O3–TeO2–ZnO glasses: fabrication, physical, structural characterization, and radiation shielding efficacy, Opt. Mater. (2021), 110757, https://doi.org/10.1016/j.optmat.2020.110757.
[17] M. Ali Mohammad, M. Bektasoglu, Comparative study of two bismuth–borate glasses in terms of gamma shielding parameters at medical diagnostic energies and neutron shielding characteristics, Mater. Chem. Phys. 255 (2020), 123609, https://doi.org/10.1016/j.matchemphys.2020.123609.
[18] M. Sayyed, Y. Rammah, A. Abouhaswa, H. Tekin, B. Elbashir, ZnO-B2O3-PbO glasses: synthesis and radiation shielding characterization, Phys. B Condens. Matter 548 (2018) 20–26, https://doi.org/10.1016/j.physb.2018.08.024.
[19] J. Liu, X. Xu, T. Zheng, Y. Guo, J. Lv, Effect of Bi2O3 content on the structure and properties of Bi2O3-B2O3-BaO-ZnO glass, J. Non-Cryst. Solids 575 (2022), 121211, https://doi.org/10.1016/j.jnoncrysol.2021.121211.
[20] E. Şakar, Ö. Özpolat, B. Alım, M. Sayyed, M. Kurudirek, Phy-X / PSD: development of a user friendly online software for calculation of parameters relevant to radiation shielding and dosimetry, Radiat. Phys. Chem. 166 (2020), 108496, https://doi.org/10.1016/j.radphyschem.2019.108496.
[21] I.I. Bashter, A.S. Makarious, E.S. Abdo, Investigation of hemati-te–serpentine and ilmenite-limonite concretes for reactorradiation shielding, Ann. Nucl. Energy 23 (1) (1996) 65–71.
[22] A.M. Ali, S.A.M. Issa, M.R. Ahmed, Y.B. Saddeek, M.H. Mohd Zaid, M. Sayed, H.H. Somaily, H.O. Tekin, H.A. Aziz Sidek, K.A. Matori, H.M.H. Zakaly, Promising applicable heterometallic Al2O3/PbO2 nanoparticles in shielding properties, J. Mater. Res. Technol. 9 (6) (2020) 13956–13962, https://doi.org/10.1016/j.jmrt.2020.09.125.
[23] A.M.A. Henaish, M. Mostafa, B.I. Salem, H.M.H. Zakaly, S.A.M. Issa, I.A. Weinstein, O.M. Hemeda, Spectral, electrical, magnetic and radiation shielding studies of Mg-doped Ni–Cu–Zn nanoferrites, J. Mater. Sci. Mater. Electron. 22 (2020) 1–13.
[24] M. Rashad, T.A. Hanafy, S.A. Issa, Structural, electrical andradiation shielding properties of polyvinyl alcohol doped withdifferent nanoparticles, J. Mater. Sci. Mater. Electron 31 (18) (2020) 15192–15197.
[25] A. Abou Elfadl, A.M. Ismail, M.I. Mohammed, Dielectric study andAC conduction mechanism of gamma irradiated nano-compo-site of polyvinyl alcohol matrix with Cd0.9Mn0.1S, J. Mater. Sci. Mater. Electron 31 (11) (2020) 8297–8307.
[26] P. Florian, N. Sadiki, D. Massiot, J.P. Coutures, 27Al NMR study of the structure of lanthanum- and yttrium-based aluminosilicateglasses and melts, J. Phys. Chem. B 111 (33) (2007) 9747–9757.
[27] G. Singh, M.K. Gupta, A.S. Dhaliwal, K.S. Kahlon, Measurement ofattenuation coefficient, effective atomic number and electron density of oxides of lanthanides by using simplified ATM-method. J. Alloy. Compd. 2015;619:356–360. S.A. Issa, Effective atomic number and mass attenuation coefficient of PbO–BaO–B2O3 glass system. Radiat. Phys. Chem. 2016;120:33–37.
[28] A.I. Elazaka, H.M. Zakaly, S.A. Issa, M. Rashad, H.O. Tekin, H.A. Saudi, et al., New approach to removal of hazardous Bypass Cement Dust (BCD) from the environment: 20$Na^{2}O$–^{20}BaCl2-(60-x)B2O3-(x)BCD glass system and optical, mechanical, structural and nuclear radiation shielding competences, J. Hazard. Mater. 403 (2021), 123738.
[29] N. Ekinci, E. Kavaz, Y. Özdemir, A study of the energy absorptionand exposure buildup factors of some anti-inflammatorydrugs, Appl. Radiat. Isot. 90 (2014) 265–273.

[30] X-rayabsorption in matter. Reengineering XCOM. Radiat. Phys. Chem. 2001;60(1–2):23–24. L. Gerward, N. Guilbert, K.B. Jensen, H. Levring, WinXCom – aprogram for calculating X-ray attenuation coefficients. Radiat. Phys. Chem. 2004;71(3–4):653–354.
[31] H.O. Tekin, E. Kavaz, E.E. Altunsoy, O. Kilicoglu, O. Agar, T.T. Erguzel, et al., An extensive investigation on gamma-ray and neutronattenuation parameters of cobalt oxide and nickel oxide sub-stituted bioactive glasses, Ceram. Int. 45 (8) (2019) 9934–9949.
[32] Y.B. Saddeek, S.A. Issa, T. Alharbi, R. Elsaman, G. Abd Elfadeel, A.M. Mostafa, et al., Synthesis and characterization of leadborate glasses comprising cement kiln dust and Bi2O3 forradiation shielding protection, Mater. Chem. Phys. 242 (2020), 122510.
[33] H.O. Tekin, S. Alomairy, M.S. Al-Buriahi, Y. Rammah, Linear/nonlinear optical parameters along with photon attenuation effectiveness of Dy3+ ions doped zinc-aluminoborosilicate glasses, Phys. Scr. 96 (2021), 065704, https://doi.org/10.1088/1402-4896/abf452.
[34] C.Y. Zhao, T.J. Lu, H.P. Hodson, J.D. Jackson, The temperature dependence of effective thermal conductivity of open-celled steel alloy foams, Mater. Sci. Eng. A 367 (2004) 123–131, https://doi.org/10.1016/j.msea.2003.10.241.